BJP BRITISH JOURNAL OF PHARMACOLOGY

BPS BRITISH PHARMACOLOGICAL SOCIETY

BJP British Journal of Pharmacology

DOI:10.1111/j.1476-5381.2010.00902.x
www.brjpharmacol.org

RESEARCH PAPER

Role of perinuclear mitochondria in the spatiotemporal dynamics of spontaneous Ca^{2+} waves in interstitial cells of Cajal-like cells of the rabbit urethra

Hikaru Hashiatni[1], Richard J Lang[2] and Hikaru Suzuki[1]

[1]*Department of Cell Physiology, Nagoya City University Graduate School of Medical Sciences, Nagoya, Japan, and* [2]*Department of Physiology, School of Biomedical Sciences, Monash University, Clayton, Victoria, Australia*

Correspondence
Hikaru Hashiatni, Department of Cell Physiology, Nagoya City University Graduate School of Medical Sciences, Nagoya 467-8601, Japan. E-mail: hasitani@med.nagoya-cu.ac.jp

Keywords:
ICC-like cell; urethra; spontaneous Ca^{2+} wave; perinuclear mitochondria; endoplasmic reticulum; inhibition of glycolysis

Received
5 February 2010
Revised
5 May 2010
Accepted
9 May 2010

BACKGROUND AND PURPOSE

Although spontaneous Ca^{2+} waves in interstitial cells of Cajal (ICC)-like cells (ICC-LCs) primarily arise from endoplasmic reticulum (ER) Ca^{2+} release, the interactions among mitochondrial Ca^{2+} buffering, cellular energetics and ER Ca^{2+} release in determining the spatiotemporal dynamics of intracellular Ca^{2+} remain to be elucidated.

EXPERIMENTAL APPROACH

Spontaneous Ca^{2+} transients in freshly isolated ICC-LCs of the rabbit urethra were visualized using fluo-4 Ca^{2+} imaging, while the intracellular distribution of mitochondria was viewed with MitoTracker Red.

KEY RESULTS

Spontaneous Ca^{2+} waves invariably originated from the perinuclear region where clusters of mitochondria surround the nucleus. Perinuclear Ca^{2+} dynamics were characterized by a gradual rise in basal Ca^{2+} that preceded each regenerative Ca^{2+} transient. Caffeine evoked oscillatory Ca^{2+} waves originating from anywhere within ICC-LCs. Ryanodine or cyclopiazonic acid prevented Ca^{2+} wave generation with a rise in basal Ca^{2+}, and subsequent caffeine evoked a single rudimentary Ca^{2+} transient. Inhibition of glycolysis with 2-deoxy-glucose or carbonyl cyanide 3-chlorophenylhydrazone, a mitochondrial protonophore, increased basal Ca^{2+} and abolished Ca^{2+} waves. However, caffeine still induced oscillatory Ca^{2+} transients. Mitochondrial Ca^{2+} uptake inhibition with RU360 attenuated Ca^{2+} wave amplitudes, while mitochondrial Ca^{2+} efflux inhibition with CGP37157 suppressed the initial Ca^{2+} rise to reduce Ca^{2+} wave frequency.

CONCLUSIONS AND IMPLICATIONS

Perinuclear mitochondria in ICC-LCs play a dominant role in the spatial regulation of Ca^{2+} wave generation and may regulate ER Ca^{2+} release frequency by buffering Ca^{2+} within microdomains between both organelles. Glycolysis inhibition reduced mitochondrial Ca^{2+} buffering without critically disrupting ER function. Perinuclear mitochondria may function as sensors of intracellular metabolites.

Abbreviations

$\Delta\Psi m$, mitochondrial inner membrane potential; 2DG, 2-deoxy-glucose; CCCP, carbonyl cyanide 3-chlorophenylhydrazone; CPA, cyclopiazonic acid; DS, dispersal solution; ER, endoplasmic reticulum; ICC-LC, interstitial cells of Cajal-like cell; SERCA, sarco-endoplasmic reticulum Ca^{2+} ATPase; STD, spontaneous transient depolarization; STIC, spontaneous inward current

Introduction

Smooth muscle of the urethra generates spontaneous tone to maintain urinary continence (Bridgewater *et al.*, 1993). This tone arises from smooth muscle bundles generating spontaneous phasic contractions triggered upon Ca^{2+} influx through L-type Ca^{2+} channels opened during the plateau phase of slow waves (Hashitani *et al.*, 1996; Hashitani and Edwards, 1999; channel nomenclature follows Alexander *et al.*, 2009). These slow waves are considered to result from the temporal summation of spontaneous transient depolarizations (STDs) that arise from the release of Ca^{2+} from intracellular stores and the opening of Ca^{2+}-activated chloride channels (Hashitani and Edwards, 1999).

STDs in the urethra appear to be generated in specialized cells that have similar morphological characteristics to interstitial cells of Cajal (ICC) in the gastrointestinal (GI) tract (Sanders *et al.*, 2006), and are clearly distinguishable from smooth muscle cells (Sergeant *et al.*, 2000). The cells can be identified by their immunereactivity to Kit antibodies, a specific marker for ICC, and thus are referred to as ICC-like cells (ICC-LCs, Hashitani and Suzuki, 2007; Lyons *et al.*, 2007). ICC-LCs in the urethra do not form an extensive network (Lyons *et al.*, 2007), nor act as a synchronous electrical pacemaker of smooth muscle activity as do ICC in the GI tract (Hashitani and Suzuki, 2007). Rather, ICC-LCs are thought to electrically drive individual smooth muscle bundles by means of their localized STD discharge, which increases the overall excitability of the urethral smooth muscle.

The development of freshly isolated single ICC-LC preparations from the rabbit urethra has confirmed many of the suppositions made from previous *in situ* experiments. Spontaneous inward currents (STICs) and their corresponding STDs have been directly demonstrated to arise from the opening of Ca^{2+}-activated Cl^- channels that are triggered by the release of stored Ca^{2+} from the endoplasmic reticulum (ER) (Sergeant *et al.*, 2000; 2001; Johnston *et al.*, 2005). Moreover, the initiation of spontaneous activity of ICC-LCs primarily depends on the Ca^{2+} release through ryanodine receptor Ca^{2+} channels in the ER membrane. Inositol trisphosphate receptor (IP_3R) Ca^{2+} channels are thought to play a fundamental role in the intracellular propagation of Ca^{2+} waves to cause a synchronous activation of the Ca^{2+}-activated chloride channels underlying slow wave generation (Johnston *et al.*, 2005).

More recently, the involvement of mitochondrial Ca^{2+} buffering in the generation of spontaneous Ca^{2+} waves and STICs has been suggested (Sergeant *et al.*, 2008). Similar cooperation between ER and mitochondria in generating spontaneous electrical and Ca^{2+} activity has been shown for ICC in the GI tract (Ward *et al.*, 2000), ICC-LCs in the gall bladder (Balemba *et al.*, 2008) and in atypical smooth muscle cells, the pacemaker cells in the renal pelvis (Hashitani *et al.*, 2009). However, what role these two distinct organelles play in the spatiotemporal dynamics of intracellular Ca^{2+} is not yet well understood. As ATP production by mitochondria is not critically involved in the generation of spontaneous Ca^{2+} waves (Ward *et al.*, 2000; Balemba *et al.*, 2008; Sergeant *et al.*, 2008), even though refilling of the ER fundamentally depends on Ca^{2+} uptake via the sarco-ER Ca^{2+} ATPase (SERCA) pump, the metabolic basis for spontaneous activity in ICC or ICC-like cells has yet to be resolved.

In the present study, spontaneous Ca^{2+} waves in ICC-LCs freshly isolated from the rabbit urethra were visualized using fluo-4 fluorescence, and their spatial relationship with the intracellular distribution of mitochondria was established with the vital mitochondria stain, MitoTracker Red. We also examined the effects of pharmacologically manipulating Ca^{2+} uptake into and release from the ER and mitochondria, as well as the effects of inhibiting glycolysis on Ca^{2+} wave generation and propagation.

Methods

Tissue preparation

All animal care and experimental procedures have been approved by the animal experimentation ethics committee of Nagoya City University. Male rabbits, weighing 2–3 kg, were killed by exsanguination under pentobarbitone anaesthesia. The urethra and bladder were removed, and the urethra was dissected free of the bladder approximately 3 cm distal to the bilateral ureteral entries. The dorsal wall of the urethra was opened longitudinally; the mucosa and periurethral connective tissues were then dissected away. Under a dissecting microscope, the most proximal part of the urethra, approximately 1 cm wide, was isolated from the remaining parts of the tissue. During preliminary experiments, ICC-LCs were most readily isolated from the longitudinal smooth muscle layer in comparison with either the circular smooth muscle layer or lamina propria. Thus, longitudinal layers were carefully dissected away from circular smooth muscle layers, and were then processed for cell isolation.

Cell isolation

Longitudinal smooth muscle portions were cut into small pieces approximately 3 × 3 mm and less than

1 mm thickness, and stored for 30 min in Ca^{2+} free HEPES-buffered dispersal solution (DS) [composition (in mM): Na^+ 126, K^+ 6, Mg^{2+} 1, Cl^- 134, glucose 10 and HEPES 10; pH adjusted to 7.4 with NaOH]. The muscle pieces were then incubated in Ca^{2+}-free DS containing 3 mg collagenase (Worthington, Lakewood, NJ, USA, type I), 0.2 mg protease (Sigma type XXIV), 2 mg BSA (Sigma, St. Louis, MO, USA) and 2 mg trypsin inhibitor (Sigma), for approximately 10 min at 37°C. The preparations were then placed in low Ca^{2+} DS ($[Ca^{2+}]$ = 100 μM) for 30 min at room temperature. Single cells were obtained by gentle agitation for 5–10 min with a wide-bore pipette; cells in suspension were transferred to glass bottom recording chambers and kept for 10–20 min at room temperature to allow adherence to the glass coverslip.

Intracellular Ca^{2+} imaging

To image the intracellular Ca^{2+} dynamics in freshly isolated ICC-LCs, cells were incubated in HEPES-buffered low-Ca^{2+} DS ($[Ca^{2+}]$ = 100 μM) containing 1 μM fluo-4 AM (special packaging, Dojindo, Kumamoto, Japan) for 5–10 min at room temperature. Following incubation, the cells were superfused with dye-free, warmed (36°C) HEPES-buffered PSS [composition (in mM): Na^+ 137.5, K^+ 5.9, Ca^{2+} 2.5, Mg^{2+} 1.2, $H_2PO_4^-$ 1.2, Cl^- 134, glucose 10 and HEPES 10; pH adjusted to 7.4 with NaOH] at a constant flow rate (about 2 mL·min^{-1}) for 30 min.

The recording chamber was mounted on the stage of an upright epifluorescence microscope (BX51WI, Olympus, Tokyo, Japan) equipped with an electron multiplier CCD camera (C9100, Hamamatsu Photonics, Hamamatsu, Japan) and a high-speed scanning polychromatic light source (C7773, Hamamatsu Photonics). Cells were viewed with a water immersion objective (LUMPlanFI x60, Olympus) and illuminated at 495 nm. The fluorescence emission was captured through a barrier filter above 515 nm, and images were obtained every 23–200 ms (frame interval) with an exposure time of 17.4–58.7 ms using a micro-photoluminescence measurement system (AQUACOSMOS, Hamamatsu Photonics). Relative amplitude of Ca^{2+} transients was expressed as the ratio (F/F_0) of the fluorescence generated by an event (F) against baseline (F_0).

Intracellular imaging of mitochondria, ER and nuclei

To assess the intracellular distribution of mitochondria or nuclei, ICC-LCs were incubated with either 10 nM MitoTracker Red (Invitrogen, Carlsbad, CA, USA) for 10 min at room temperature, or 100 nM Hoechst 33342 (Invitrogen) for 5 min at room temperature respectively. ICC-LCs were then superfused with dye-free, warmed (36°C) HEPES-buffered PSS ($[Ca^{2+}]$ = 2.5 mM) at a constant flow rate (about 2 mL·min^{-1}) for 20 min. Images of fluorescent organelles were acquired using the same epifluorescence microscope and objectives as above. MitoTracker Red was excited at 580 nm, and emission was collected at 600 nm. Hoechst 33342 was excited at 360 nm, and emission was detected at 460 nm. Only ICC-LCs in which staining of either mitochondria or nuclei did not disrupt the generation of spontaneous Ca^{2+} waves were included for spatial Ca^{2+} dynamics analysis.

To assess the intracellular distribution of ER relative to the mitochondria distribution, ICC-LCs which had been stained with MitoTracker Red were subsequently incubated with 1 μM ER-Tracker Blue-White DPX (Invitrogen) for 15 min at room temperature. ICC-LCs were then observed immediately after incubation in the probe solution, as staining was reduced considerably on its removal (Cole *et al.*, 2000). ER-Tracker Blue-White DPX was excited at 360 nm, and emission was detected at 560 nm.

Data analysis

The following parameters of spontaneous Ca^{2+} transients were measured: peak amplitude, measured as the value from the resting level to the peak of events; half-amplitude duration, measured as the time between 50% peak amplitude on the rising and falling phases; and frequency, which was defined as an average over 3 or 5 min of recording. In some cells, the conducting velocity of spontaneous Ca^{2+} waves, the rate of initial Ca^{2+} rise or the decay of Ca^{2+} transients was also calculated.

Measured values were expressed as mean ± SD. Statistical significance was tested using paired Student's t-test, and considered significant if $P < 0.05$. The number of cells examined was expressed by n, while N indicates the number of animals.

Materials

Drugs used were caffeine, cyclopiazonic acid (CPA), carbonyl cyanide 3-chlorophenylhydrazone (CCCP), 2-deoxy-glucose (2DG), nicardipine, nifedipine (from Sigma-Aldrich), CGP37157, RU360 and ryanodine (from Calbiochem, La Jolla, CA, USA). 2DG and RU360 were dissolved in distilled water, and CPA, CCCP, CGP37157 and nicardipine were dissolved in dimethyl sulphoxide (DMSO). Nifedipine was dissolved in ethanol. Caffeine was directly dissolved in PSS. Glucose-free/2DG solution was prepared by replacing glucose with 2DG. Nominally, a Ca^{2+}-free solution was prepared by omitting $CaCl_2$ from PSS. The final concentration of DMSO or ethanol in the PSS did not exceed 1:1000.

Results

Intracellular distribution of mitochondria and ER

ICC-LCs freshly isolated from the longitudinal smooth muscle layer of the rabbit urethra had a variety of morphologies that were distinct from the smooth muscle cells that had a smooth spindle-shaped cell body. ICC-LCs had a long, thin cell body with either several distinct angles (42.0% of n = 278 cells from N = 48 rabbits, Figure 1Aa), spiky processes (31.2%, Figure 1Ba) or a short spindle-shaped cell body with many spiky processes (26.8%, Figure 2Ca). In all ICC-LCs, nuclei were readily viewed under bright field illumination (Figure 1Ab), and their location could be confirmed by staining with Hoechst 33342 (Figure 1Ba–c). Upon staining with MitoTracker Red, mitochondria were observed to be preferentially clustered around the nucleus (Figure 1Ab,c and Bb,c), while other short filamentous mitochondria were scattered along the long axis of the cell body in a daisy chain arrangement (Figure 1Ad).

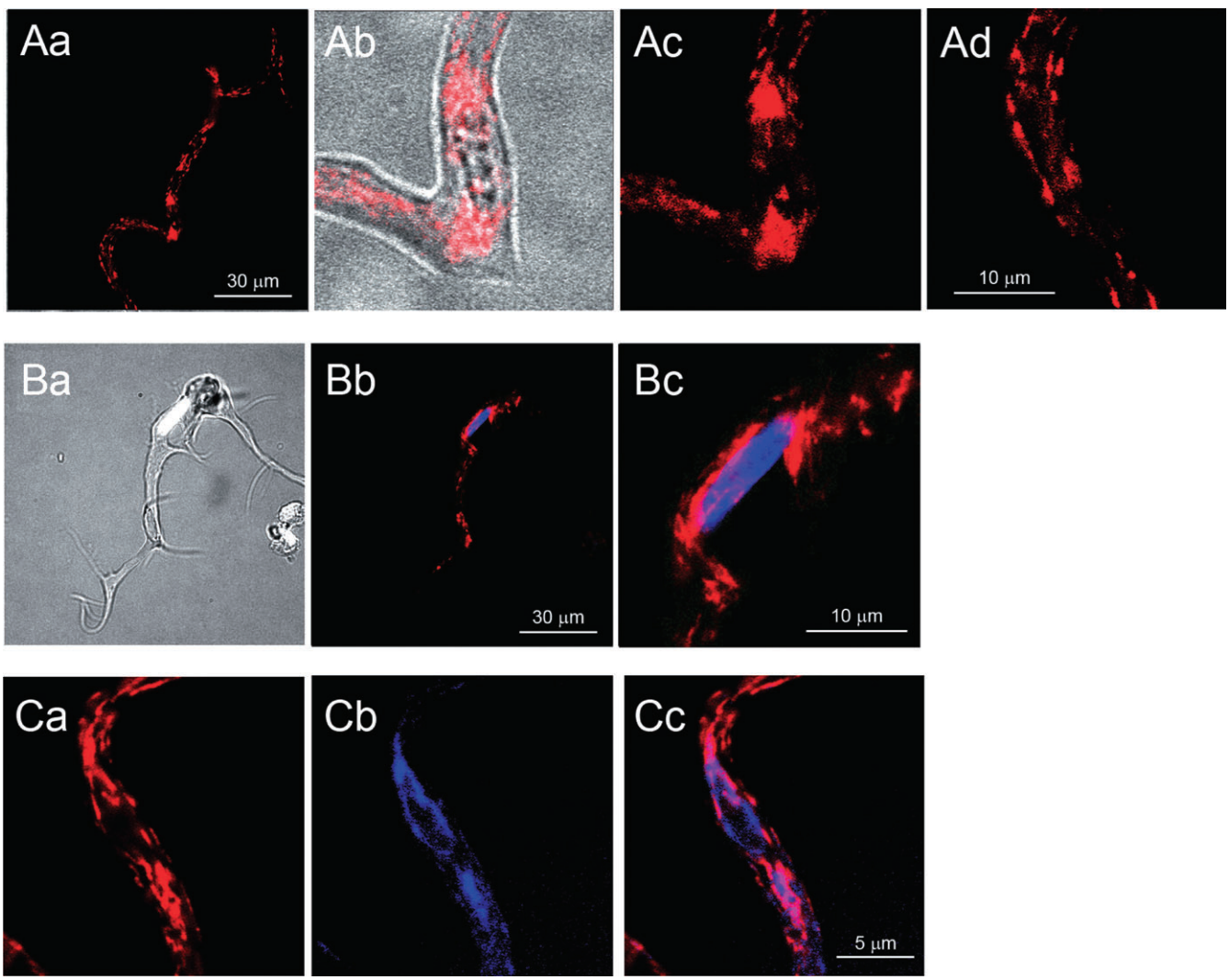

Figure 1

Intracellular distribution of mitochondria and ER in urethral ICC-like cells. Fluorescent images of an ICC-LC loaded with MitoTracker-Red (Aa). Perinuclear clusters of mitochondria are evident on both sides of the nucleus in an enlarged overlay image of bright field and MitoTracker-Red (Ab). Enlarged images indicate perinuclear clusters of mitochondria (Ac), while filamentous mitochondria are distributed in the cell periphery (Ad). An overlay image of another ICC-LC with a bright field view and Hoechst 33342 staining (Ba), and a corresponding overlay fluorescent image with Hoechst 33342 and MitoTracker-Red staining (Bb). An enlarged overlay image of perinuclear region illustrating that clusters of mitochondria surround the nucleus (Bc). In a different ICC-LC, in which perinuclear clusters of mitochondria were stained with MitoTracker-Red (Ca), the ER, stained with ER-Tracker, was also distributed around the nucleus (Cb). An overlay image showing a close apposition of perinuclear mitochondria with ER (Cc).

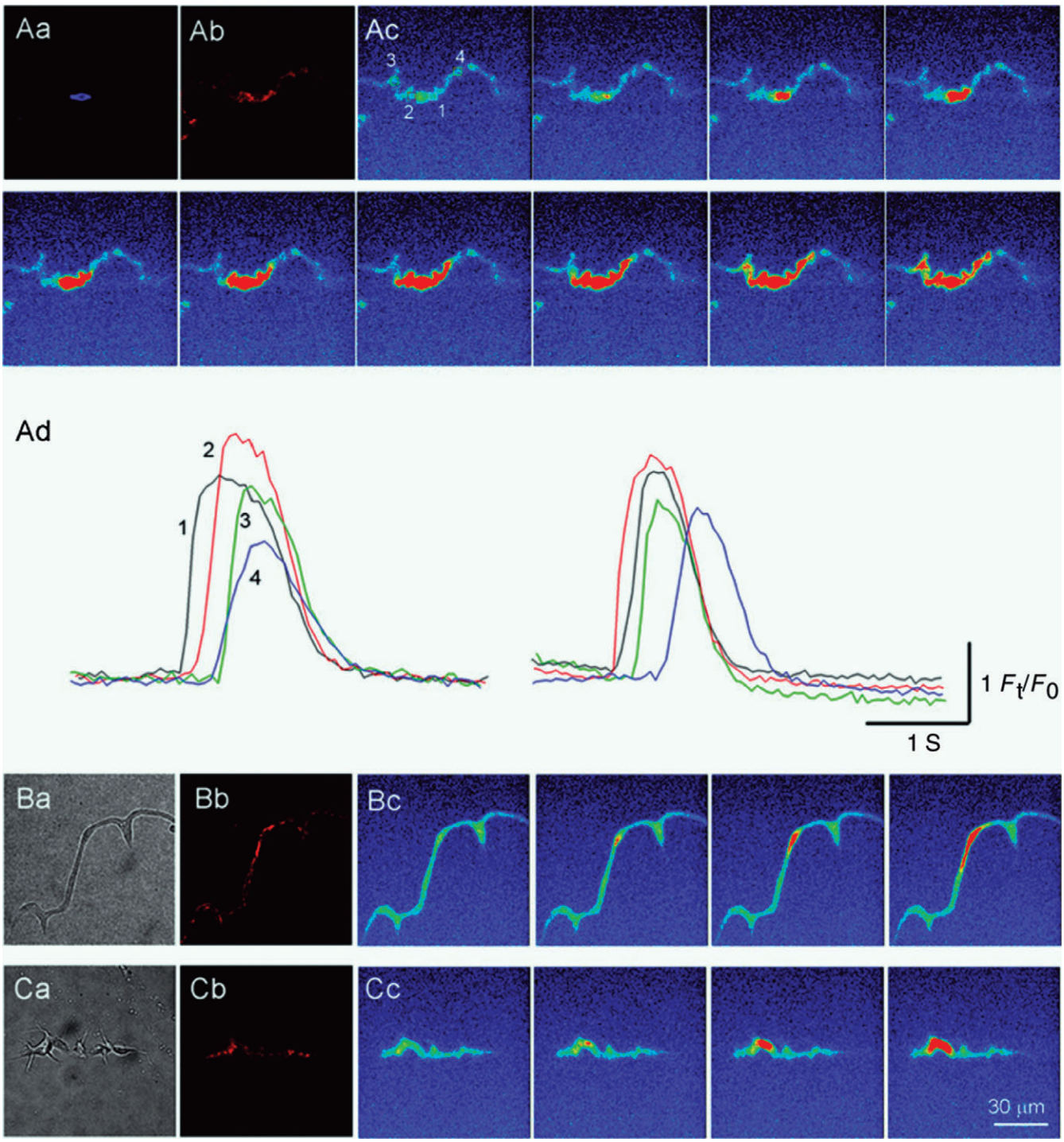

Figure 2

Spatial relationship between perinuclear mitochondria and spontaneous Ca^{2+} waves in urethral ICC-LCs. Fluorescent images of an ICC-LC loaded with Hoechst Blue (Aa) and MitoTracker-Red (Ab). Sequential fluo-4 fluorescent images of a spontaneous Ca^{2+} wave (Ac) with frame interval of 100 ms. Temporal sequence of Ca^{2+} transients captured from four areas in ICC-LC (Ad). Spontaneous Ca^{2+} waves originated from either side of perinuclear mitochondria and spread to the cell periphery. Bright field (Ba) and corresponding MitoTracker-Red fluorescent (Bb) images of another ICC-LC. Sequential fluo-4 fluorescent images showing a Ca^{2+} wave originating from perinuclear mitochondria (Bc). Bright field (Ca) and corresponding MitoTracker-Red (Cb) images of a different ICC-LC. Sequential fluo-4 fluorescent images showing a Ca^{2+} wave originating from perinuclear mitochondria (Cc).

The intracellular distribution of ER was also examined by staining ICC-LCs with ER-Tracker Blue-White DPX. In ICC-LCs that expressed perinuclear mitochondrial staining (Figure 1Ca), ER was also clustered around the nucleus (Figure 1Cb), demonstrating the co-localization of mitochondria and ER in perinuclear regions of ICC-LCs (Figure 1C,c, n = 23, N = 8).

Spatial dynamics of Ca^{2+} waves

All experiments were carried out in the presence of nifedipine (1 μM) or nicardipine (1 μM) to exclude a possible contribution of Ca^{2+} influx through L-type Ca^{2+} channels to the intracellular Ca^{2+} dynamics in ICC-LCs.

Two hundred sixteen ICC-LCs isolated from 48 animals exhibited spontaneous Ca^{2+} waves that invariably originated from the perinuclear region. In Figure 2, three representative ICC-LCs firing spontaneous Ca^{2+} waves have also been stained to illustrate their spatial distribution of mitochondria. In an ICC-LC in which mitochondria mostly surrounded the nucleus (Figure 2Aa,b), spontaneous Ca^{2+} waves originated from either side of the perinuclear region (Figure 2Ac; Supporting Information Video Clip S1). Not only did these Ca^{2+} transients travel to the periphery on the same side of the nucleus from which they originated, they also readily travelled across the nucleus and spread towards the periphery of the opposite side (Figure 2Ad). In ICC-LCs that had either long, thin cell bodies (Figure 2B) or had short spindle cell bodies with many spiky branches (Figure 2C), mitochondria were clustered around the perinuclear regions, as well as scattered throughout the periphery (Figure 2B). In both cell types, spontaneous Ca^{2+} waves originated from the perinuclear regions and propagated to their cell periphery. Thus, regardless of cell morphology or the location of the nucleus, spontaneous Ca^{2+} waves invariably originated from the perinuclear regions, suggesting that perinuclear mitochondria may play an important role in determining the spatiotemporal dynamics of Ca^{2+} waves in ICC-LCs.

Properties of perinuclear and peripheral Ca^{2+} transients

The triggering of spontaneous perinuclear Ca^{2+} waves in some cells was characterized by an initial gradual rise in Ca^{2+} level that preceded individual Ca^{2+} transients (52.5% of n = 216 cells, Figure 3A). In 13.9% of cells, perinuclear Ca^{2+} waves were preceded by a number of Ca^{2+} transients which gradually grew in amplitude, all of which were triggered from a relatively stable (flat) baseline (Figure 3C). The remaining 37% of cells exhibited a combination of these two discharge patterns such that increasing amplitude Ca^{2+} transients were recorded on a rising baseline (Figure 3B) before the main Ca^{2+} wave discharge. In peripheral regions of ICC-LCs, small amplitude non-propagating Ca^{2+} transients were often recorded (Figure 3D). These small non-propagating Ca^{2+} transients invariably failed to fire during the period following the passing of a propagating Ca^{2+} waves (Figure 3D). Alternatively, the cell periphery could be abruptly 'awakened' from quiescence by Ca^{2+} waves that propagated from the perinuclear regions.

Spontaneous Ca^{2+} waves were generated in perinuclear regions at a frequency of 2.6 ± 1.2 min^{-1}, and propagated to the cell periphery at a velocity of 68.8 ± 25.2 $\mu m \cdot ms^{-1}$ (n = 51, N = 23). Perinuclear Ca^{2+} transients had an amplitude of 1.94 ± 0.75 F_t/F_0 and a half-width of 1.1 ± 0.38 s (n = 51, N = 23). Perinuclear Ca^{2+} transients had a faster falling phase in comparison to peripheral Ca^{2+} transients: the decay time constant (τ) for perinuclear Ca^{2+} transients was 410 ± 128 ms and significantly smaller than the τ value for peripheral Ca^{2+} transients (550 ± 174 ms; $P < 0.05$, n = 45, N = 20).

Effects of caffeine on Ca^{2+} dynamics

Caffeine (10 mM) evoked Ca^{2+} waves that gradually reduced in amplitude and prevented the further generation of spontaneous Ca^{2+} waves (Figure 4, n = 7, N = 6), suggesting that continuous activation of ryanodine receptors results in a functional depletion of Ca^{2+} in the ER. The initial perinuclear Ca^{2+} transient induced by caffeine had an amplitude of 2.3 ± 0.51 F_t/F_0, which was 108.5 ± 5.6% of the amplitude of their corresponding control spontaneous Ca^{2+} transients. In ICC-LCs that remained quiescent (n = 3, N = 3) or generated only small Ca^{2+} fluctuations (n = 2, N = 2), caffeine evoked oscillatory Ca^{2+} waves. It should be noted that caffeine-induced Ca^{2+} waves originated from sites anywhere along the length of each ICC-LC, and thus perinuclear regions did not act as a dominant site of the origin of caffeine-induced Ca^{2+} waves (Figure 4).

Role of ER Ca^{2+} handlings and extracellular Ca^{2+} in Ca^{2+} wave generation

The role of Ca^{2+} handling by ER in the temporal dynamics of perinuclear Ca^{2+} transients was examined by manipulating ER Ca^{2+} sequestration and release, using CPA and ryanodine respectively. The ER Ca^{2+} content remaining after exposure to either CPA or ryanodine was estimated by exposing cells to caffeine (10 mM).

CPA (10 μM) increased the basal Ca^{2+} level by 0.36 ± 0.11 F_t/F_0 and prevented the further generation of spontaneous Ca^{2+} waves (Figure 5Aa, n = 10,

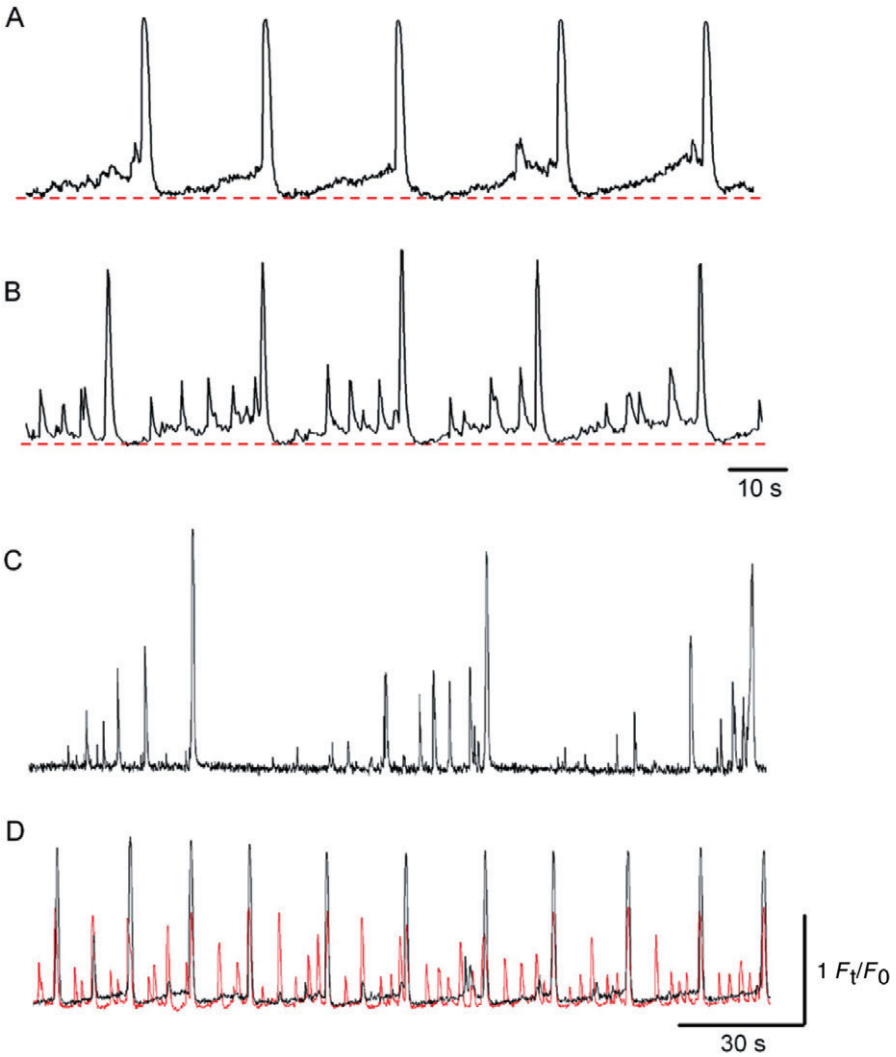

Figure 3

Properties of perinuclear Ca^{2+} transients in ICC-LCs. In an ICC-LC, perinuclear Ca^{2+} transients were characterized by an initial gradual rise in basal Ca^{2+} that preceded each regenerative Ca^{2+} transient (A). In another ICC-LC, a gradual rise in basal Ca^{2+} that was superimposed by ongoing Ca^{2+} fluctuations preceded each Ca^{2+} transient (B). The time-scale for (B) also refers to (A). In a different ICC-LC, each Ca^{2+} transient was followed by a quiescent period and subsequent increasing amplitude small Ca^{2+} fluctuations that preceded the next Ca^{2+} transient (C). A simultaneous recording of perinuclear and peripheral Ca^{2+} transients in an ICC-LC (D). In the cell periphery (red), small Ca^{2+} fluctuations were generated, while regenerative Ca^{2+} transients were triggered by Ca^{2+} waves propagated from perinuclear regions. The time-scale for (D) also refers to (C); the fluorescence scale for (D) refers to all traces.

N = 9). Subsequent exposure to caffeine (10 mM) caused a single, rudimentary Ca^{2+} transient that had an absolute amplitude of 0.21 ± 0.08 F_t/F_0. The peak value of Ca^{2+} recorded upon exposure to caffeine was 25.1 ± 5.3% of the untreated spontaneous Ca^{2+} transients. These results are summarized in Figure 5Ab, and suggest that CPA prevention of Ca^{2+} waves results from the depletion of ER Ca^{2+} content, and that continuous Ca^{2+} uptake by SERCA is fundamental in maintaining both ER levels of releasable Ca^{2+} and a low basal cytosolic Ca^{2+}.

Ryanodine (100 μM, n = 8, N = 6) abolished spontaneous Ca^{2+} waves with a rise in the basal Ca^{2+} level of 0.26 ± 0.11 F_t/F_0 (Figure 5Ba). The subsequent application of caffeine evoked only a single small Ca^{2+} transient that had an amplitude of 0.2 ± 0.06 F_t/F_0 and a peak value that was 26.4 ± 6.7% of control spontaneous Ca^{2+} transients. These results are summarized in Figure 5Bb, and suggest that the ryanodine-induced rises in basal Ca^{2+} level may be due to the activation of ryanodine receptors that results in a critical reduction of releasable Ca^{2+} from the ER.

Although perinuclear Ca^{2+} transient generation relied on ER Ca^{2+} handing, nominally Ca^{2+}-free PSS readily prevented the generation of Ca^{2+} transients

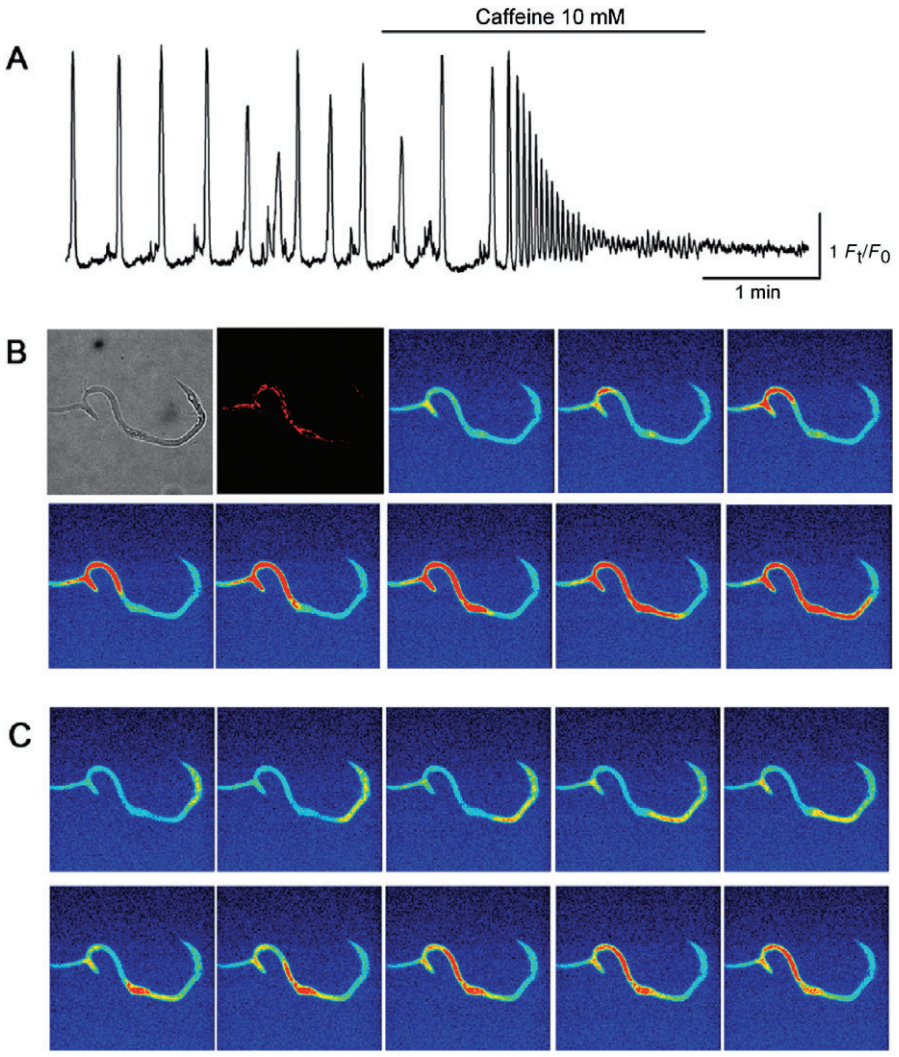

Figure 4

Effects of caffeine on Ca^{2+} dynamics in ICC-LCs. In an ICC-LC that generated spontaneous Ca^{2+} waves, caffeine (10 mM) evoked oscillatory Ca^{2+} transients (A). The amplitude of caffeine-induced Ca^{2+} transients gradually reduced until the generation of spontaneous Ca^{2+} waves ceased. In another ICC-LC which expressed MitoTracker Red fluorescence in its perinuclear regions, caffeine triggered Ca^{2+} waves from distinct peripheral sites that travelled across the nucleus towards the other side of the cell periphery (B, C).

associated with a fall in the basal Ca^{2+} level of 0.31 ± 0.10 F_t/F_0 (n = 5, N = 4; Figure 5C). Upon returning to normal PSS, both spontaneous Ca^{2+} transients and basal Ca^{2+} levels were immediately restored.

Role of mitochondrial Ca^{2+} handlings in Ca^{2+} wave generations

The role of mitochondrial Ca^{2+} uptake in the temporal dynamics of spontaneous perinuclear Ca^{2+} waves was examined by disrupting the mitochondrial inner membrane potential ($\Delta\Psi m$), using the protonophore CCCP, which results in an inhibition of Ca^{2+} influx. The Ca^{2+} content of the ER under these conditions was again estimated by exposing cells to caffeine.

CCCP (1 μM) increased basal Ca^{2+} levels by 0.40 ± 0.12 F_t/F_0 and prevented the generation of spontaneous Ca^{2+} waves (Figure 6Aa). Subsequent exposure to caffeine (10 mM) induced oscillatory Ca^{2+} transients with a mean amplitude of 1.68 ± 0.12 F_t/F_0; the peak value of the caffeine-induced Ca^{2+} transient was not significantly different (102 ± 5%, $P > 0.05$, n = 8, N = 6) from the control spontaneous Ca^{2+} transients. These results are summarized in Figure 6Ab and suggest that disruption of the mitochondrial inner membrane potential was not associated with a critical suppression of SERCA or ER Ca^{2+} storage. More likely, abolition of Ca^{2+} waves induced by CCCP resulted from a reduction of Ca^{2+} influx into mitochondria subsequent to the collapse of $\Delta\Psi m$.

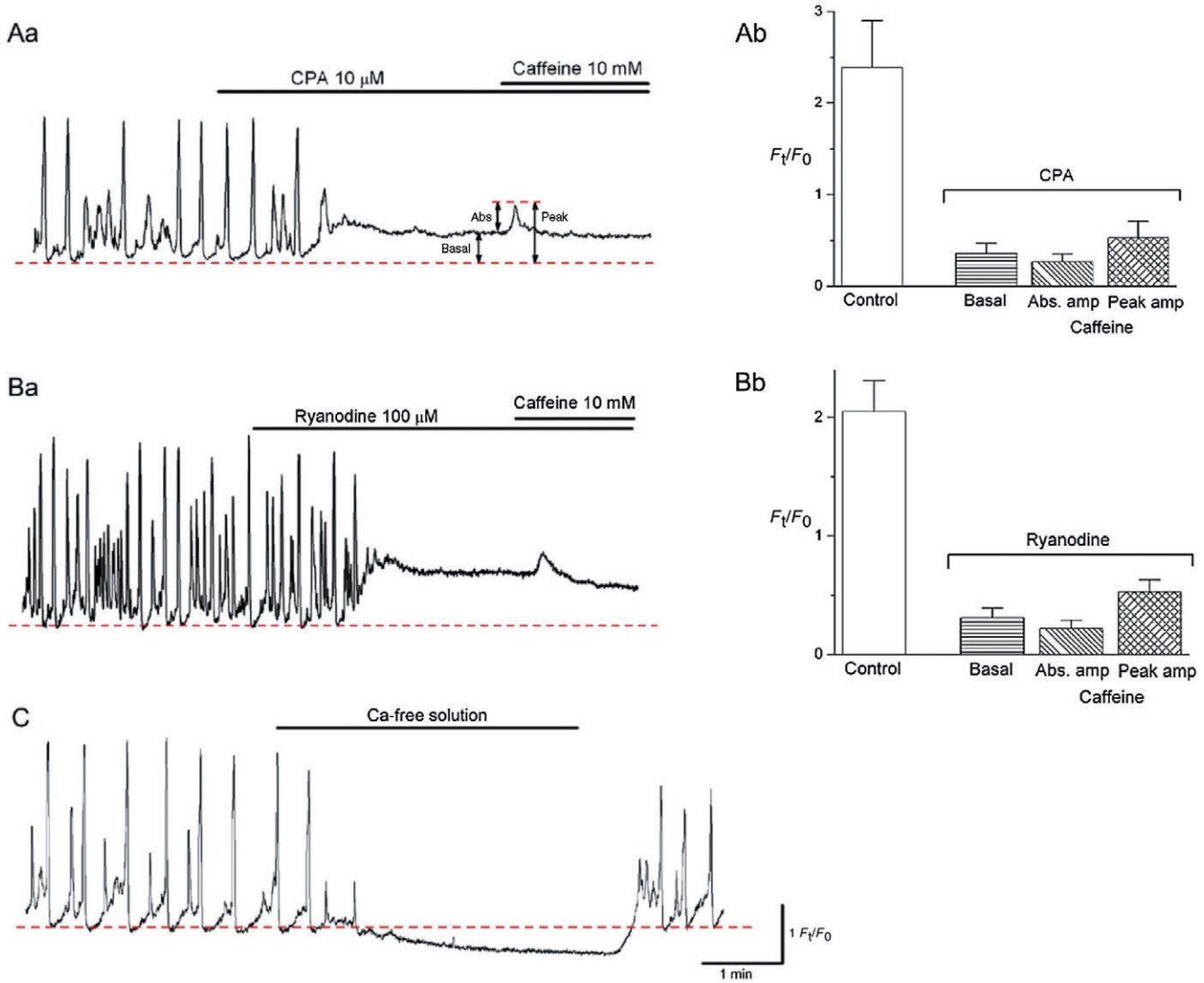

Figure 5

Effects of CPA, ryanodine and Ca^{2+}-free solution on perinuclear Ca^{2+} transients in ICC-LCs. CPA (10 μM) prevented the generation of spontaneous Ca^{2+} transients with a rise in the basal Ca^{2+} (Aa). Subsequent application of caffeine evoked a single rudimentary Ca^{2+} transient. The results obtained from 10 ICC-LCs are summarized in (Ab). In another spontaneously active ICC-LC, ryanodine (100 μM) abolished spontaneous Ca^{2+} transients with an increase in basal Ca^{2+} (Ba). The subsequent addition of caffeine caused only a single small Ca^{2+} transient. The results obtained from six ICC-LCs were summarized in (Bb). In (Ab) and (Bb), control indicates the amplitude of spontaneous Ca^{2+} transients, and basal, Abs.amp and peak amp indicate the corresponding values shown in (Aa). In a different ICC-LC, switching from PSS to nominally Ca^{2+}-free solution caused a reduction in basal Ca^{2+} and cessation of Ca^{2+} transients that recovered upon the re-admission of extracellular Ca^{2+} (C). The scale bars for (C) also refer to Aa and Ba.

The role of mitochondrial Ca^{2+} influx in spontaneous Ca^{2+} dynamics was more specifically investigated using RU360, an inhibitor of the mitochondrial Ca^{2+} uniporter. In six (N = 4) out of nine ICC-LCs (N = 6), RU360 (10 μM for 5–10 min) increased the basal Ca^{2+} level and prevented the generation of spontaneous Ca^{2+} waves, although some small, non-propagating Ca^{2+} fluctuations remained (Figure 6B). In the three other (N = 3) ICC-LCs, RU360 reduced the frequency of spontaneous Ca^{2+} waves and increased the occurrence of small Ca^{2+} fluctuations, but did not prevent Ca^{2+} wave generation even after 30 min of exposure (Figure 6C).

In seven ICC-LC (N = 6), CGP37157, an inhibitor of the mitochondrial Na^+ : Ca^{2+} exchanger, reduced the frequency of spontaneous Ca^{2+} waves by suppressing the initial gradual rise in basal Ca^{2+} level that preceded Ca^{2+} transients, but did not abolish Ca^{2+} waves even after 30 min (Figure 6D). The slope of the initial Ca^{2+} rises was 0.022 ± 0.005 F_t/F_0 s^{-1} in control, 0.009 ± 0.004 F_t/F_0 s^{-1} in CGP37157 (P <

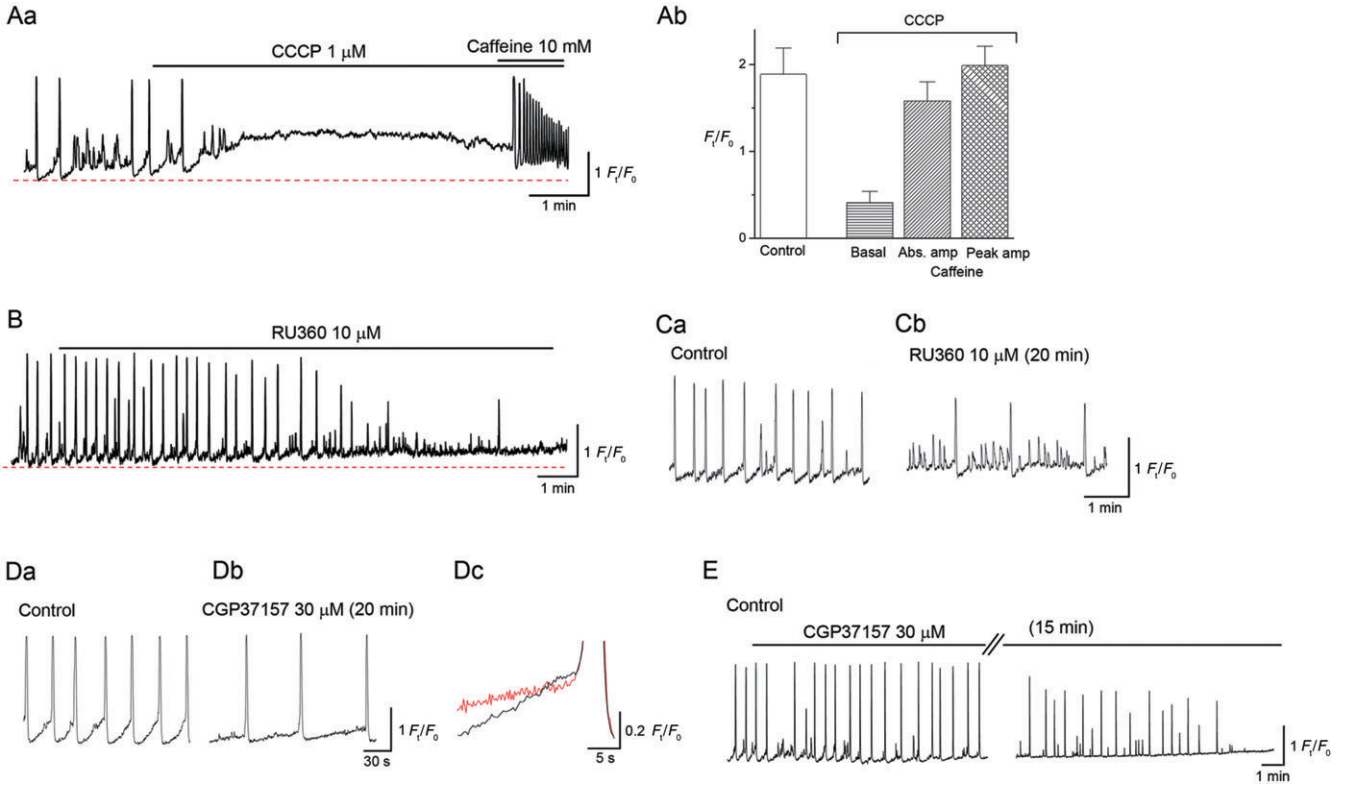

Figure 6

Effects of CCCP, RU360 and CGP37157 on perinuclear Ca^{2+} transients in ICC-LCs. In an ICC-LC developing spontaneous Ca^{2+} transients, CCCP (1 μM) prevented the generation of Ca^{2+} transients with a rise in the basal Ca^{2+} (A). Subsequent caffeine exposure evoked oscillatory Ca^{2+} transients. The results obtained from eight ICC-LCs are summarized in (B). In another spontaneously active ICC-LC, RU360 (10 μM) abolished spontaneous Ca^{2+} transients with an increase in basal Ca^{2+} (C). In a different ICC-LC, RU360 reduced the frequency of spontaneous Ca^{2+} transients and induced small Ca^{2+} fluctuations (Ca,b). CGP37157 (30 μM) reduced the frequency of spontaneous Ca^{2+} transients (Da,b) by suppressing the initial gradual rise in Ca^{2+} (Dc). In a different ICC-LC, CGP37157 eventually abolished spontaneous Ca^{2+} transients with an increase in basal Ca^{2+} (E).

0.05, $n = 7$). In three other cells ($N = 2$), CGP37157 (30 μM) reduced the frequency of spontaneous Ca^{2+} waves and eventually prevented Ca^{2+} wave generation after 15–25 min in a manner associated with an increase in basal Ca^{2+} level (Figure 6E).

Role of glycolysis in the generation of Ca^{2+} waves

Because reducing the electrical driving force for ATP synthesis with CCCP did not critically reduce the Ca^{2+} content of the ER (Figure 5), mitochondrial ATP production may not be fundamental for a functioning SERCA, at least over the short period of our experiments. This view is supported by the recent finding that oligomycin, a blocker of mitochondrial ATP synthetase, did not affect spontaneous Ca^{2+} waves in urethral ICC-LCs (Sergeant *et al.*, 2008).

To investigate the role of glycolysis in both ATP production and mitochondrial substrates supply, the effects of 2DG on ICC-LC Ca^{2+} waves were examined in 15 ICC-LCs ($N = 12$). 2DG (10 mM) prevented the generation of spontaneous Ca^{2+} waves within 5–20 min, which was associated with a rise in basal Ca^{2+} level. These effects were readily reversible upon returning to normal glucose containing PSS (Figure 7A). However, in nine ICC-LCs ($N = 9$), the subsequent addition of caffeine (10 mM) in the continuing presence of 2DG still induced oscillatory Ca^{2+} transients, suggesting that inhibition of glycolysis did not critically reduce the ER Ca^{2+} content. The rise in basal Ca^{2+} in 2DG suggests that reducing the supply of mitochondrial substrates is vital to maintaining $\Delta\Psi m$, which, in turn, is essential in keeping the cytosolic Ca^{2+} concentration at low levels.

Discussion and conclusions

In ICC-LCs freshly isolated from longitudinal smooth muscle layer of the rabbit urethra, clusters of mitochondria surround the nucleus, while fila-

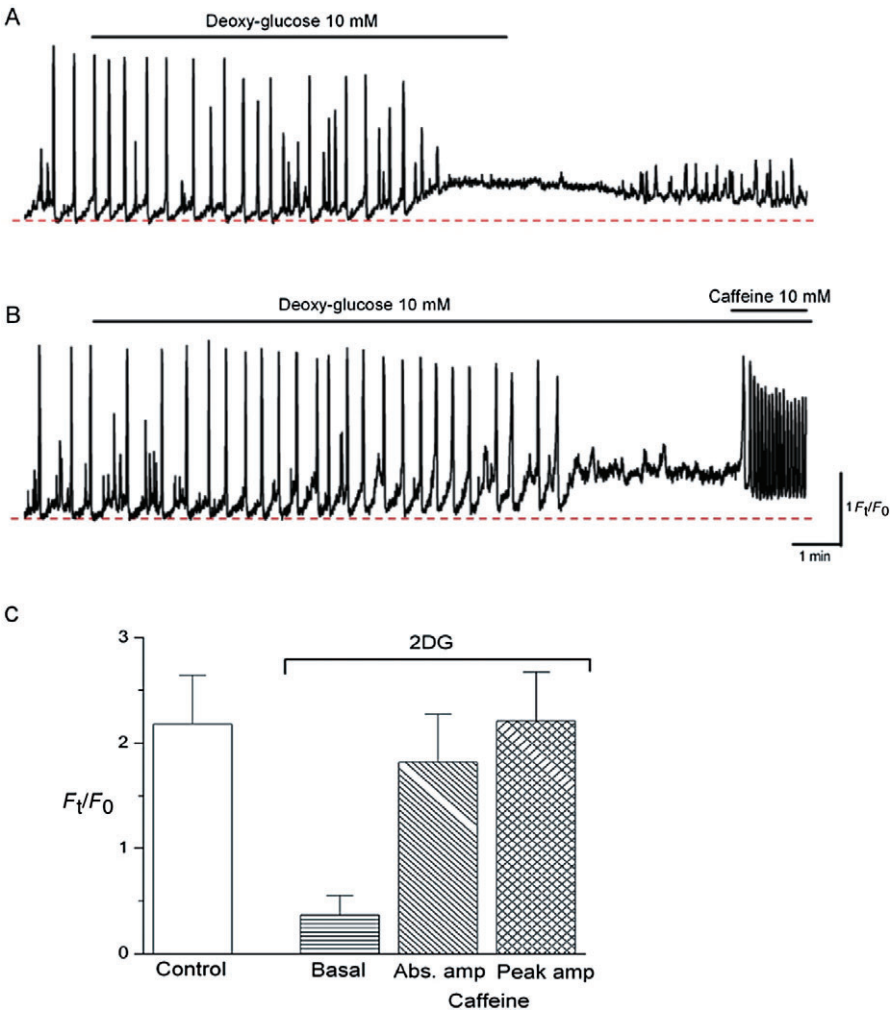

Figure 7

Effects of 2DG on perinuclear Ca^{2+} transients in ICC-LCs. In an ICC-LC that displayed spontaneous Ca^{2+} transients, 2DG increased the basal Ca^{2+} which suppressed the generation of spontaneous Ca^{2+} transients (A). Upon switching from 2DG/glucose-free PSS back to normal PSS, Ca^{2+} gradually returned to the original level and small Ca^{2+} fluctuations re-appeared. In another ICC-LC, 2DG increased the basal Ca^{2+} which eventually abolished Ca^{2+} wave generation (B). Upon the cessation of Ca^{2+} transients, a subsequent exposure to caffeine evoked oscillatory Ca^{2+} transients. Effects of 2DG and caffeine obtained from nine ICC-LCs are summarized in (C).

mentous mitochondria were scattered throughout the cell periphery. Spontaneous Ca^{2+} waves invariably originated from the perinuclear regions where these mitochondrial clusters were situated, and propagated to the cell periphery, suggesting that perinuclear mitochondria may play a fundamental role in determining spatial dynamics of Ca^{2+} in ICC-LCs. Spontaneous Ca^{2+} waves in ICC-LCs are associated with the generation of STDs (Sergeant *et al.*, 2000) that transmit to adjacent smooth muscle cells to depolarize their membranes (Hashitani and Suzuki, 2007). Besides the generation of electrical activity, intracellular Ca^{2+} signalling is also crucially involved in many other cell functions, including gene transcription, protein synthesis and cell proliferation, and thus spatio-temporal Ca^{2+} dynamics have to be finely controlled (Bootman *et al.*, 2001). The initiation of spontaneous Ca^{2+} waves in perinuclear regions may indicate a cross-talk between the nucleus and mitochondria.

Mitochondrial Ca^{2+} uptake is also critical in regulating mitochondrial oxidative metabolism, that is, ATP synthesis, because several mitochondrial dehydrogenases are sensitive to mitochondrial Ca^{2+} concentrations (Robb-Gaspers *et al.*, 1998; Jouaville *et al.*, 1999). In parotid acinar cells, in which a majority of mitochondria are located around the nucleus, agonist-evoked Ca^{2+} waves are delayed as they propagate through the nucleus, and are accompanied by a substantial increase in NADH autofluorescence (Bruce *et al.*, 2004). It has been suggested that perinuclear mitochondria may have a potential

role in shaping nuclear Ca^{2+} signals, but more importantly, drive mitochondrial metabolism to generate ATP close to the nucleus (Bruce *et al.*, 2004). A similar tight energetic transport between the perinuclear mitochondria and the nucleus in urethra ICC-LCs may explain the lack of inhibition of SERCA after pharmacological disruption of mitochondrial function in the present experiments.

The Ca^{2+} release from ER through ryanodine receptors has been considered to be the primary step of Ca^{2+} dynamics in ICC-LCs, while IP_3-dependent Ca^{2+} release may be required in the propagation or coordination of Ca^{2+} waves (Johnston *et al.*, 2005). The importance of mitochondrial Ca^{2+} buffering in regulating temporal Ca^{2+} dynamics in ICC-LCs is now becoming apparent as a reduction of mitochondrial Ca^{2+} uptake results in the cessation of spontaneous Ca^{2+} waves, while the acceleration of Ca^{2+} uniporter increases Ca^{2+} wave frequency (Sergeant *et al.*, 2008). Because mitochondria Ca^{2+} buffering appears to be important in regulating the temporal dynamics of Ca^{2+} in ICC-LCs, the far higher density of mitochondria in perinuclear regions in comparison with the cell periphery may indicate a larger Ca^{2+} buffering capacity in restricted areas surrounding the nucleus. This view may be supported by the smaller decay time constant for perinuclear Ca^{2+} transients than that for peripheral Ca^{2+} transients, as well as the recording of small Ca^{2+} fluctuations more frequently in the cell periphery. In our experiments, blockade of the Ca^{2+} uniporter with bath applied RU 360 took longer to exert its inhibitory action on Ca^{2+} waves, and did not consistently abolish their generation, in comparison to when cells were dialysed with RU360 (Sergeant *et al.*, 2008). Nevertheless, non-propagating Ca^{2+} fluctuations in the perinuclear region were increased in cells treated with RU360 and re-appeared more quickly than the appearance of spontaneous Ca^{2+} waves, upon the wash-out of 2DG with normal glucose-containing PSS. Therefore, perinuclear mitochondria may buffer Ca^{2+} concentrations in microdomains, and play a role in restricting Ca^{2+} release from the ER and allowing sufficient ER Ca^{2+} sequestration, necessary for the generation of regenerative Ca^{2+} waves. In cardiac cells, inhibition of mitochondrial Ca^{2+} uptake results in an increase in the frequency and duration of Ca^{2+} sparks (Pacher *et al.*, 2002). Because of the low affinity of the mitochondrial Ca^{2+} uniporter, Ca^{2+} uptake preferentially operates in Ca^{2+}-loaded microdomains in close proximity to ER Ca^{2+} release channels. The possibility of such microdomains in urethral ICC-LCs is suggested by our demonstration that the ER in ICC-LCs stained with ER-Tracker displayed a similar perinuclear distribution as mitochondria. Such close contacts and functional interactions between mitochondria and ER/SR have been reported in other cell types (Rizzuto *et al.*, 1998; Szalai *et al.*, 2000). Although we have not investigated the intracellular distribution of ryanodine receptors, perinuclear clusters of ryanodine receptors have been reported in ICC-LCs of the rabbit portal vein (Harhun *et al.*, 2006). In the cell periphery where the mitochondria : ER ratio may be lower than perinuclear regions so that microdomains are not so well established, Ca^{2+} release and uptake from ryanodine receptors may be predominantly regulated by the ER itself, with only a smaller participation of mitochondrial Ca^{2+} buffering. Upon stimulation with caffeine, an increased sensitivity of ryanodine receptors to cytosolic Ca^{2+} may overcome ER luminal inhibition and initiate regenerative Ca^{2+} waves from multiple sites within ICC-LCs.

The Ca^{2+} release from ER through ryanodine receptors is regulated by both cytosolic and luminal Ca^{2+} concentration (Györke and Györke, 1998). In the present study, CPA inhibition of SERCA prevented Ca^{2+} wave generation, which was associated with a rise in basal Ca^{2+} level, and the subsequent caffeine caused a single rudimentary Ca^{2+} release from ER. Thus, ER function appears to require continuous Ca^{2+} uptake by SERCA, and reduced SERCA activity instantly results in a substantial fall of ER Ca^{2+} contents. In HeLa cells, thapsigargin caused a rapid, substantial fall in ER content (Arnaudeau *et al.*, 2001). When ER Ca^{2+} content falls, caffeine-induced increases in the sensitivity of ryanodine receptors to cytosolic Ca^{2+} may not be able to cause any further Ca^{2+} release, presumably via their inhibition by low luminal Ca^{2+} in the ER store. Ryanodine also prevented the generation of spontaneous Ca^{2+} waves, which was associated with a rise in basal Ca^{2+}. Subsequent cell exposure to caffeine evoked only a single, small Ca^{2+} transient that was equivalent to those observed upon CPA treatment, suggesting ryanodine may effectively diminish ER Ca^{2+} content by forming a long-lasting, subconductance state of the Ca^{2+}-releasing channels (Rousseau *et al.*, 1987).

Inhibition of mitochondrial Ca^{2+} release by CGP37157 suppressed the initial gradual rise in basal Ca^{2+} and reduced the frequency of Ca^{2+} waves, suggesting that mitochondrial Ca^{2+} efflux through the $Na^+ : Ca^{2+}$ exchanger may contribute to the gradual rise in basal Ca^{2+}. Such gradual rises in basal Ca^{2+} that precede each Ca^{2+} transient are observed in ICC-LCs of the rabbit portal vein in which spontaneous Ca^{2+} waves also originate from the perinuclear regions (Harhun *et al.*, 2006). Transfer of Ca^{2+} from mitochondria to the ER as the mitochondrial $Na^+ : Ca^{2+}$ exchanger releases Ca^{2+} close to SERCA,

and its importance in the ER Ca^{2+} refilling has been reported in HeLa cells (Arnaudeau *et al.*, 2001; Ishii *et al.*, 2006) and HUVECs (Malli *et al.*, 2005). In HeLa cells, ER regions close to mitochondria release sites maintain a higher Ca^{2+} content than regions lacking mitochondria due to this substantial mobilization of Ca^{2+} from mitochondria to ER (Arnaudeau *et al.*, 2001). Consistent with our observations, CGRP37157 has been shown to take some 20 min to reduce the frequency of Ca^{2+} waves in the gall bladder (Balemba *et al.*, 2008). Because mitochondrial Ca^{2+} efflux may also depend on Na^+-independent Ca^{2+} efflux, the effects of CGRP37157, and therefore the relative contribution of mitochondrial $Na^+ : Ca^{2+}$ exchanger to mitochondrial Ca^{2+} efflux, may vary between cells. In three ICC-LCs, CGP37157 eventually suppressed spontaneous Ca^{2+} waves in a manner that was associated with a rise in the basal Ca^{2+} level, suggesting that an excessive rise in mitochondrial Ca^{2+} content subsequent to $Na^+ : Ca^{2+}$ exchanger inhibition may result in the suppression of mitochondrial Ca^{2+} uptake (Chalmers and McCarron, 2009) as it relies on both $\Delta\Psi m$ and the Ca^{2+} gradient across the inner membrane.

Although spontaneous Ca^{2+} transients in the urethral ICC-LCs primarily rely on Ca^{2+} mobilization through the ER in association with mitochondrial Ca^{2+} buffering, nominally Ca^{2+}-free solution readily prevented the generation of Ca^{2+} transients associated with a reduction in the basal Ca^{2+}. This is consistent with the previous demonstration that the frequency of Ca^{2+} transients in ICC-LCs critically depends on the extracellular Ca^{2+} concentrations (Johnston *et al.*, 2005). Previous studies also indicate that the $Na^+ : Ca^{2+}$ exchanger on the plasma membrane operating in reverse mode, rather than store-operated Ca^{2+} entry, plays an important role in maintaining cytosolic Ca^{2+} concentrations at levels which allow the refilling of the ER (Bradley *et al.*, 2005; 2006). Because low subplasmalemmal Ca^{2+} concentrations are necessary before Ca^{2+} influx can take place through the plasmalemmal $Na^+ : Ca^{2+}$ exchanger, mitochondria may also play a role in buffering Ca^{2+} microdomains around these exchangers to regulate the rate of ER refilling.

Because SERCA activity is vital in maintaining ER function as a primary step of Ca^{2+} wave generation, continuous and sufficient ATP must be supplied to SERCA by intracellular energy production systems. In atypical smooth muscle cells of the mouse renal pelvis, inhibition by oligomycin of mitochondrial ATP synthesis reduced the frequency of spontaneous Ca^{2+} transients arising from Ca^{2+} movement between the ER and mitochondria (Hashitani *et al.*, 2009). However, oligomycin did not prevent the generation of Ca^{2+} waves in urethral ICC-LCs (Johnston *et al.*, 2005), suggesting that mitochondrial ATP production may not be fundamental in maintaining SERCA function in the ER membrane. In HeLa cells in which ATP is mainly generated by glycolysis, mitochondrial ATP generation also does not contribute significantly to SERCA function (Jouaville *et al.*, 1999; Arnaudeau *et al.*, 2001). In the present experiments and consistent with this notion, caffeine was capable of generating oscillatory Ca^{2+} transients after the cessation of spontaneous Ca^{2+} waves with CCCP. Although inhibition of glycolysis, with 2DG and glucose omission, abolished Ca^{2+} waves, the subsequent application of caffeine still evoked oscillating Ca^{2+} transients, suggesting that inhibition of glycolysis did not critically reduce ATP supply to SERCA, and that the effects of 2DG resulted from a reduced mitochondrial Ca^{2+} uptake subsequent to the reduced availability of mitochondrial substrates. Because the supply of mitochondrial substrates, particularly glucose, is fundamental in maintaining mitochondrial respiration and thus the inner $\Delta\Psi m$, inhibition of glycolysis would be expected to subsequently reduce Ca^{2+} uptake that relies on this voltage gradient. ICC-LCs may store substantial amounts of creatine phosphate by consuming ATP produced by their numerous mitochondria, and thus may be able to maintain SERCA activity for short periods during a reduction in the supply of glucose and oxygen (i.e. during ischaemia). Thus, perinuclear mitochondria in ICC-LCs may sense cellular metabolic demands, as well as local metabolic supply, by altering their Ca^{2+}-buffering capacity, and play a key role in determining spatio-temporal Ca^{2+} dynamics that critically link a number of diverse cellular functions.

Acknowledgements

This project was supported by a Grant-in-Aid for Scientific Research (B) from JSPS to H.H. (no. 19390418) and by the NHMRC (Australia) to R.J.L.

Conflict of interest

The authors state no conflict of interest.

References

Alexander SPH, Mathie A, Peters JA (2009). *Guide to Receptors and Channels (GRAC)*, 4th edn. Br J Pharmacol 158 (Suppl. 1): S1–S254.

Arnaudeau S, Kelley WL, Walsh JV Jr, Demaurex N (2001). Mitochondria recycle Ca^{2+} to the endoplasmic reticulum and prevent the depletion of neighboring endoplasmic reticulum regions. J Biol Chem 276: 29430–29439.

Balemba OB, Bartoo AC, Nelson MT, Mawe GM (2008). Role of mitochondria in spontaneous rhythmic activity and intracellular calcium waves in the guinea pig gallbladder smooth muscle. Am J Physiol Gastrointest Liver Physiol 29: G467–G476.

Bootman MD, Lipp P, Berridge MJ (2001). The organisation and functions of local Ca^{2+} signals. J Cell Sci 114: 2213–2222.

Bradley E, Hollywood MA, McHale NG, Thornbury KD, Sergeant GP (2005). Pacemaker activity in urethral interstitial cells is not dependent on capacitative calcium entry. Am J Physiol Cell Physiol 289: C625–C632.

Bradley E, Hollywood MA, Johnston L, Large RJ, Matsuda T, Baba A *et al*. (2006). Contribution of reverse Na^{+}–Ca^{2+} exchange to spontaneous activity in interstitial cells of Cajal in the rabbit urethra. J Physiol 574: 651–661.

Bridgewater M, MacNeil HF, Brading AF (1993). Regulation of urethral tone in pig urethral smooth muscle. J Urol 150: 223–228.

Bruce JL, Giovannucci DR, Blinder G, Shuttleworth TJ, Yule DI (2004). Modulation of $[Ca^{2+}]_i$ signaling dynamics and metabolism by and metabolism by perinuclear mitochondria in mouse parotid acinar cells. J Biol Chem 279: 12909–12917.

Chalmers S, McCarron JG (2009). Inhibition of mitochondrial calcium uptake rather than efflux impedes calcium release by inositol-1,4,5-trisphosphate-sensitive receptors. Cell Calcium 46: 107–113.

Cole L, Davies D, Hyde GJ, Ashford AE (2000). ER-Tracker dye and BODIPY-brefeldin A differentiate the endoplasmic reticulum and Golgi bodies from the tubularvacuole system in living hyphae of *Pisolithus tinctorius*. J Microscopy 197: 239–248.

Györke I, Györke S (1998). Regulation of the cardiac ryanodine receptor channel by luminal Ca^{2+} involves luminal Ca^{2+} sensing sites. Biophys J 75: 2801–2810.

Harhun M, Gordienko D, Kryshtal D, Pucovský V, Bolton T (2006). Role of intracellular stores in the regulation of rhythmical $[Ca^{2+}]_i$ changes in interstitial cells of Cajal from rabbit portal vein. Cell Calcium 40: 287–298.

Hashitani H, Edwards FR (1999). Spontaneous and neurally activated depolarizations in smooth muscle cells of the guinea-pig urethra. J Physiol 514: 459–470.

Hashitani H, Van Helden DF, Suzuki H (1996). Properties of spontaneous depolarizations in circular smooth muscle cells of rabbit urethra. Br J Pharmacol 118: 1627–1632.

Hashitani H, Suzuki H (2007). Properties of spontaneous Ca^{2+} transients recorded from interstitial cells of Cajal-like cells of the rabbit urethra *in situ*. J Physiol 583: 505–519.

Hashitani H, Lang RJ, Mitsui R, Mabuchi Y, Suzuki H (2009). Distinct effects of CGRP on typical and atypical smooth muscle cells involved in generating spontaneous contractions in the mouse renal pelvis. Br J Pharmacol 158: 2030–2045.

Ishii K, Hirose K, Iino M (2006). Ca^{2+} shuttling between endoplasmic reticulum and mitochondria underlying Ca^{2+} oscillations. EMBO Rep 7: 390–396.

Johnston L, Sergeant GP, Hollywood MA, Thornbury KD, McHale NG (2005). Calcium oscillations in interstitial cells of the rabbit urethra. J Physiol 565: 449–461.

Jouaville LS, Pinton P, Bastianutto C, Rutter GA, Rizzuto R (1999). Regulation of mitochondrial ATP synthesis by calcium: evidence for a long-term metabolic priming. Proc Natl Acad Sci U S A 96: 13807–13812.

Lyons AD, Gardiner TA, McCloskey KD (2007). Kit-positive interstitial cells in the rabbit urethra: structural relationships with nerves and smooth muscle. BJU Int 99: 687–694.

Malli R, Frieden M, Trenker M, Graier WF (2005). The role of mitochondria for Ca^{2+} refilling of the endoplasmic reticulum. J Biol Chem 280: 12114–12122.

Pacher P, Thomas AP, Hajnóczky G (2002). Ca^{2+} marks: miniature calcium signals in single mitochondria driven by ryanodine receptors. Proc Natl Acad Sci U S A 99: 2380–2385.

Rizzuto R, Pinton P, Carrington W, Fay FS, Fogarty KE, Lifshitz LM *et al*. (1998). Close contacts with the endoplasmic reticulum as determinants of mitochondrial Ca^{2+} responses. Science 280: 1763–1766.

Robb-Gaspers LD, Burnett P, Rutter GA, Denton RM, Rizzuto R, Thomas AP (1998). Integrating cytosolic calcium signals into mitochondrial metabolic responses. EMBO J 17: 4987–5000.

Rousseau E, Smith JS, Meissner G (1987). Ryanodine modifies conductance and gating behavior of single Ca^{2+} release channel. Am J Physiol 253: C364–C368.

Sanders KM, Koh SD, Ward SM (2006). Interstitial cells of Cajal as pacemakers in the gastrointestinal tract. Annu Rev Physiol 68: 307–343.

Sergeant GP, Hollywood MA, McCloskey KD, Thornbury KD, McHale NG (2000). Specialised pacemaking cells in the rabbit urethra. J Physiol 526: 359–366.

Sergeant GP, Hollywood MA, McCloskey KD, McHale NG, Thornbury KD (2001). Role of IP3 in modulation of spontaneous activity in pacemaker cells of rabbit urethra. Am J Physiol Cell Physiol 280: C1349–C1356.

Sergeant GP, Bradley E, Thornbury KD, McHale NG, Hollywood MA (2008). Role of mitochondria in modulation of spontaneous Ca^{2+} waves in freshly dispersed interstitial cells of Cajal from the rabbit urethra. J Physiol 586: 4631–4642.

Szalai G, Csordás G, Hantash BM, Thomas AP, Hajnóczky G (2000). Calcium signal transmission between ryanodine receptors and mitochondria. J Biol Chem 275: 15305–15313.

Ward SM, Ordög T, Koh SD, Baker SA, Jun JY, Amberg G *et al*. (2000). Pacemaking in interstitial cells of Cajal depends upon calcium handling by endoplasmic reticulum and mitochondria. J Physiol 525: 355–361.

Supporting information

Additional supporting information may be found in the online version of this article.

Video Clip S1 An ICC-LC was loaded with fluo-4 (1 μM), and then the mitochondria were stained with MitoTracker Red (10 nM). Fluorescence images of the ICC-LC showing the intracellular distribution of mitochondria were superimposed over the fluo-4 Ca^{2+} fluorescence movie. Note that a non-propagating Ca^{2+} transient appears in the cell periphery on the left side, while the propagating Ca^{2+} wave originated from the perinuclear mitochondria cluster on the right side of the nucleus.

Please note: Wiley-Blackwell are not responsible for the content or functionality of any supporting materials supplied by the authors. Any queries (other than missing material) should be directed to the corresponding author for the article.